



A 6.5-kb intergenic structural variation enhances P450-mediated resistance to pyrethroids in malaria vectors lowering bed net efficacy

Leon M. J. Mugenzi^{1,2,3}  | Benjamin D. Menze^{1,2} | Magellan Tchouakui² | Murielle J. Wondji^{1,2} | Helen Irving¹ | Micareme Tchoupo² | Jack Hearn¹  | Gareth D. Weedall^{1,4} | Jacob M. Riveron^{1,2} | Fidelis Cho-Ngwa³ | Charles S. Wondji^{1,2}

¹Vector Biology Department, Liverpool School of Tropical Medicine, Liverpool, UK

²Centre for Research in Infectious Diseases (CRID), Yaoundé, Cameroon

³Department of Biochemistry and Molecular Biology, Faculty of Science, University of Buea, Buea, Cameroon

⁴School of Natural Sciences and Psychology, Liverpool, John Moores University, Liverpool, UK

Correspondence

Leon M. J. Mugenzi and Charles S. Wondji, Vector Biology Department, Liverpool School of Tropical Medicine, Liverpool, UK. Emails: leon.mugenzi@crid-cam.net; charles.wondji@lstm.ac.uk

Funding information

Wellcome Trust, Grant/Award Number: 101893/Z/13/Z and 217188/Z/19/Z

Abstract

Elucidating the complex evolutionary armory that mosquitoes deploy against insecticides is crucial to maintain the effectiveness of insecticide-based interventions. Here, we deciphered the role of a 6.5-kb structural variation (SV) in driving cytochrome P450-mediated pyrethroid resistance in the malaria vector, *Anopheles funestus*. Whole-genome pooled sequencing detected an intergenic 6.5-kb SV between duplicated CYP6P9a/b P450s in pyrethroid-resistant mosquitoes through a translocation event. Promoter analysis revealed a 17.5-fold higher activity ($p < .0001$) for the SV-carrying fragment than the SV-free one. Quantitative real-time PCR expression profiling of CYP6P9a/b for each SV genotype supported its role as an enhancer because SV+/SV+ homozygote mosquitoes had a significantly greater expression for both genes than heterozygotes SV+/SV- (1.7- to 2-fold) and homozygotes SV-/SV- (4- to 5-fold). Designing a PCR assay revealed a strong association between this SV and pyrethroid resistance (SV+/SV+ vs. SV-/SV-; odds ratio [OR] = 2,079.4, $p < .001$). The 6.5-kb SV is present at high frequency in southern Africa (80%–100%) but absent in East/Central/West Africa. Experimental hut trials revealed that homozygote SV mosquitoes had a significantly greater chance to survive exposure to pyrethroid-treated nets (OR 27.7; $p < .0001$) and to blood feed than susceptible mosquitoes. Furthermore, mosquitoes homozygote-resistant at the three loci (SV+/CYP6P9a_R/CYP6P9b_R) exhibited a higher resistance level, leading to a far superior ability to survive exposure to nets than those homozygotes susceptible at the three loci, revealing a strong additive effect. This study highlights the important role of structural variations in the development of insecticide resistance in malaria vectors and their detrimental impact on the effectiveness of pyrethroid-based nets.

KEYWORDS

Anopheles funestus, bed net, insecticide resistance, structural variant

1 | INTRODUCTION

Malaria control programmes rely heavily on insecticide-based vector control interventions including the mass distribution of long-lasting insecticidal nets (LLINs) impregnated with pyrethroids (Bhatt et al., 2015). Unfortunately, the increased use of LLINs over the years has contributed, among other factors, to the selection of pyrethroid-resistant mosquitoes (Barnes, et al., 2017). The widespread resistance to insecticides in major malaria vectors including *Anopheles gambiae* and *Anopheles funestus* is probably one of the main factors behind the recent increase in malaria cases across the world, from 214 million in 2015 to 219 million in 2017 (WHO, 2018) or the stagnation of such control efforts (WHO, 2019). Such growing resistance reports call for urgent action to implement suitable resistance management strategies to reduce the impact on the effectiveness of current and future insecticide-based tools, as highlighted by the WHO global plan for insecticide resistance management (WHO, 2012). Elucidating the molecular and genetic basis of insecticide resistance is a key step to understanding factors driving resistance and to design diagnostic tools to better detect and track the spread of such resistance in the field as well as better assess its impact on the effectiveness of control tools (WHO, 2012).

The two major insecticide resistance mechanisms are target-site resistance and metabolic resistance. Target-site resistance mechanisms including knockdown resistance (*kdr*) in the sodium channel gene are well characterized in most mosquito species (Martinez-Torres et al., 1998). However, for other species such as *A. funestus*, *kdr* is absent with resistance mainly conferred by metabolic resistance (Irving & Wondji, 2017). Three classes of enzymes mainly confer metabolic resistance, notably cytochrome P450 monooxygenases (P450s), glutathione S-transferases and esterases (Hemingway & Ranson, 2000). However, the molecular drivers of metabolic resistance have been more difficult to decipher due to the greater complexity of this mechanism with several genes involved and various molecular processes potentially implicated. Nevertheless, progress has been made recently in elucidating the molecular basis of metabolic resistance in malaria vectors. For example, amino acid changes associated with the increased metabolic activity of detoxification genes have been detected notably in the *GSTe2* gene, with L119F detected in *A. funestus* (Riveron et al., 2014) and I114T in *A. gambiae* (Mitchell et al., 2012). The L119F-*GSTe2* was confirmed to confer cross-resistance to pyrethroids and DDT (dichlorodiphenyltrichloroethane) (Riveron et al., 2014). An allelic variation of detoxification genes has also been shown to confer insecticide resistance as described in the case of the P450 genes *CYP6P9a* and *CYP6P9b* (Ibrahim et al., 2015) and for *GSTe2* in the dengue vector *Aedes aegypti* (Lumjuan et al., 2011). Recently, causative mutations located in the *cis*-regulatory region of key P450 genes were shown to drive over-expression of the P450s *CYP6P9a* (Weedall et al., 2019) and *CYP6P9b* (Mugenzi et al., 2019) in *A. funestus*. Moreover, evidence

that copy number variation of detoxification genes was also playing a role in the observed insecticide resistance in mosquitoes was shown in the *A. gambiae* and *A. coluzzii* (Lucas et al., 2019). Additionally, key transcription binding factors, notably Maf-S/CncC, have been associated with insecticide resistance in major malaria vectors. In *A. funestus*, a major structural variation (SV) in the shape of a 6.5-kb insertion was reported in pyrethroid resistance mosquitoes in the intergenic regions of two P450s (*CYP6P9a* and *CYP6P9b*) (Weedall et al., 2019), raising the prospect that such structural variation could also be an key factor driving metabolic resistance in mosquitoes. Establishing the potential role of such SVs could help to elucidate the molecular basis of resistance and also design robust diagnostic tools to detect and track resistance in the field for current and future insecticides.

Therefore, to elucidate the potential role of structural variation in pyrethroid resistance, we assess the contribution of the 6.5-kb insertion in the vicinity of key P450 resistance genes in resistant *A. funestus* mosquitoes. We demonstrate using functional assays and genotype/phenotype studies that the 6.5-kb insertion has a key role in the over-expression of P450 resistance genes. We designed a PCR (polymerase chain reaction)-based diagnostic that allows us to track this SV-based resistance and use it to show that this 6.5-kb insertion acts as an enhancer significantly contributing to increase pyrethroid resistance and to exacerbate the loss of efficacy of long-lasting insecticidal nets against malaria vectors.

2 | MATERIALS AND METHODS

2.1 | Mosquito laboratory strains and field populations

Two *Anopheles funestus* laboratory colonies of FUM0Z-R and FANG, which are resistant and susceptible to pyrethroids respectively, were used (Hunt et al., 2005). FUM0Z-R originates from Mozambique while FANG is from Angola. Available DNA samples from previous studies including F_8 generation samples derived from the reciprocal crosses between the FUM0Z and FANG (Wondji et al., 2009) were used. Additionally, field-collected mosquito samples from several countries across Africa were also used for genotyping, including Democratic Republic of Congo (DRC) (2015) and Cameroon (2016) for central Africa, Ghana (2014) for West Africa, Uganda (2014) and Tanzania (2015) for East Africa, and Zambia (2015), Malawi (2014) and Mozambique (2016) for Southern Africa. These field samples were collected indoor using electric aspirators as previously described (Weedall et al., 2019).

Furthermore, reciprocal crosses between FUM0Z-R and FANG were carried out to assess the correlation between the 6.5-kb SV and the pyrethroid resistance phenotype. The genetic crosses also reduced the bias due to the difference in background. To perform these crosses, 30 FUM0Z-R males and 30 virgin FANG females were allowed to mate and the eggs reared to the next

generation, and adults of the following generations intercrossed up to F_6 .

2.2 | Screening of the 6.5-kb SV from whole-genome sequences from different regions of Africa

The sequencing data obtained by pooling DNA from several mosquitoes (Pool-Seq) for several populations of *A. funestus* (Malawi, Ghana, Benin, Cameroon, Uganda, Mozambique, DRC Kinshasa and DRC Mikalay) were analysed to confirm the presence and distribution of the 6.5-kb insert Africa-wide following the protocol described by Weedall et al. (2020). Initial processing and quality assessment of the sequence data was performed as described by Weedall et al. (2019). Pool-Seq R1/R2 read pairs and R0 reads were aligned to the reference sequence using BOWTIE2 (Langmead & Salzberg, 2012). Variant calling was carried out using SNVER version 0.5.3, with default parameters (Wei et al., 2011). Single nucleotide polymorphisms (SNPs) were filtered to remove those with total coverage depth <10 and more than the 95th percentile of the distribution of the mean depth across SNPs for each sample, as the allele frequency estimates could be inaccurate due to low coverage or misaligned paralogous sequence, respectively.

2.3 | Comparative amplification and sequencing of the CYP6P9a and CYP6P9b intergenic region between FUMOS-R and FANG

The Livak protocol (Livak, 1984) was used to extract DNA from mosquito samples. The extracted DNA was quantified using a NanoDrop lite spectrophotometer (Thermo Scientific). The intergenic region between CYP6P9a and CYP6P9b was amplified for both the pyrethroid-resistant laboratory strain FUMOS-R and the FANG pyrethroid-susceptible laboratory strain. The intergenic region for FANG was amplified using primers 6P9a5F and GAP3R (Appendix S1) using 1 U KAPA Taq polymerase (Kapa Biosystems) in 1× buffer A, 25 mM $MgCl_2$, 25 mM dNTPs and 10 mM of each primer. This was used to constitute a 15- μ L PCR mix using the following conditions: initial denaturation step of 3 min at 95°C, followed by 35 cycles of 30 s at 94°C, 2 min at 58°C and 60 s at 72°C, with 10 min at 72°C for final extension. The FUMOS-R was amplified with primers GAP1F and GAP3R (S1) using Phusion high-fidelity DNA polymerase (Thermo Scientific). The mix was made using GC buffer, 3% DMSO (dimethyl sulphoxide), 25 mM dNTPs, 10 mM of each primer and DNA from FUMOS as template. The PCR conditions were as follows: 10 min pre-denaturation at 98°C, 35 cycles of 10 s denaturation at 98°C, 30 s annealing at 62°C, 4 min extension at 72°C and a final extension at 72°C for 10 min. The PCR product was run on a 1% gel and visualized on an ENDURO GDS (Labnet) UV transilluminator. The PCR product was gel purified and ligated to PJET1.2 blunt end vector and sequenced. Sequencing data were analysed with BIOEDIT (Hall, 1999).

2.4 | Assessment of the transcriptional activity of the 6.5-kb SV using luciferase assay

2.4.1 | Cloning of the intergenic CYP6P9a-CYP6P9b for promoter activity assay

The 8.2-kb intergenic region of CYP6P9a and CYP6P9b of the FUMOS-R colony was amplified using primers 6P9bUTR8.2F (CGAGCTCGTAAGTAACACACAAAATGGT) and 6P9aUTR8.2R (CGGCTAGCCGATTTCGTTCCGCAATTCCA), as described above and DNA from FUMOS-R as a template. The recombinant plasmid was digested with restriction enzymes Sac1 and Nde1 and subcloned in pGL3 Basic luciferase vector (Promega).

2.4.2 | Luciferase reporter assay

The transfection and the luciferase assay was done as previously described (Weedall et al., 2019) using *A. gambiae* 4a-2 cell line (MRA-917 MR4, ATCC). Due to the large difference in size between the recombinant promoter constructs, an equimolar amount of each construct was used for the transfection. Luciferase assay compared the 8.2-kb intergenic region of FUMOS-R to the 0.8-kb CYP6P9a promoter constructs for FUMOS-R and FANG. Five independent transfections were carried out. The 0.8-kb CYP6P9a recombinant promoter construct of FUMOS-R contained the core promoter of CYP6P9a before the insertion point. Briefly, 600 ng of each promoter construct was transfected using the effectene transfection reagent (Qiagen). Two additional plasmids were used, the LRIM promoter construct which served as a positive control, and the actin-Renilla internal control which is used for normalization. A luminometer (EG & G Berthold) was used to measure luciferase activity 2 days after transfection.

2.5 | Design of a simple PCR assay to detect the 6.5-kb SV and analysis of its association with pyrethroid resistance

To allow a simple identification of the samples containing the 6.5-kb insertion, a PCR was designed to discriminate between mosquitoes with the 8.2-kb (FUMOS-R) and 1.7-kb (FANG) CYP6P9a and CYP6P9b intergenic region. Briefly, three primers were designed: two (FG_5F: CTTCACGTCAAAGTCCGTAT and FG_3R: TTTCGGAAAACATCCTCAA) at regions flanking the insertion point and a third primer (FZ_INS5R: ATATGCCACGAAGGAAGCAG) in the 6.5-kb insertion. One unit of KAPA Taq polymerase (Kapa Biosystems) in 1× buffer A, 25 mM $MgCl_2$, 25 mM dNTPs and 10 mM of each primer was used to constitute a 15- μ L PCR mix using the following conditions: initial denaturation step of 3 min at 95°C, followed by 35 cycles of 30 s at 94°C, 30 s at 58°C and 60 s at 72°C, with 10 min at 72°C for final extension. The amplicon was resolved on a 1.5% agarose gel stained with Midori Green Advance

DNA Stain (Nippon genetics Europe GmbH) and revealed on a UV transilluminator.

To assess the ability of the assay to discriminate between mosquitoes with the SV and those without, the assay was tried on genomic DNA extracted from 48 FUM0Z-R and 50 FANG female mosquitoes. Next, we used F_8 mosquitoes from the FUM0Z-R and FANG crossing which had been exposed to permethrin 0.75% at two different exposure times (30 and 180 min) using the standard WHO bioassay protocol. Mortality was recorded 24 hr after exposure and samples were categorized into two groups: highly resistant for those alive after 180 min of exposure and highly susceptible for those dead after 30 min. The samples were genotyped for the 6.5-kb SV to assess the correlation between the 6.5-kb SV and the insecticide susceptibility phenotype.

2.6 | Correlation between the 6.5-kb PCR assay and the *CYP6P9a/b* PCR-RFLP

The efficacy of the newly designed PCR for the 6.5-kb SV was compared by using PCR-RFLP (restriction fragment length polymorphism) methods for detecting the *CYP6P9a*- and *CYP6P9b*-resistant allele to check the association between the 6.5-kb SV and each of the P450s and also for the combined effect of these three markers, as described previously (Mugenzi et al., 2019; Weedall et al., 2019). DNA samples from previous studies were used as test materials to compare the three assays.

2.7 | Assessment of the enhancer's effect of the 6.5-kb SV on the expression of nearby genes using qRT-PCR

Structural variants are known to have the propensity to impact the expression of nearby genes on the same chromosome. To investigate the potential enhancer's effect of the 6.5-kb on the expression of *CYP6P9a* and *CYP6P9b*, mosquitoes of the F_2 generation from the FUM0Z-R and FANG crosses were used to generate the various genotypes of the 6.5-kb SV. Total RNA was extracted from the F_2 generation of FUM0Z-R and FANG crosses, which had been genotyped using the newly designed 6.5-kb SV detection PCR and grouped into three sets: homozygous for the 6.5-kb SV (SV+/SV+), heterozygous (SV+/SV-) and homozygous without the SV (SV-/SV-). DNA was extracted from the legs. Briefly, four to six legs were pulled from each mosquito and placed in a 1.5-ml tube. Then, 25 μ l of 1 \times PCR buffer B (Kapa Biosystems) prewarmed at 65°C was added and the legs were ground. The tubes were then centrifuged at 18,928 g for 2 min. The samples were then incubated at 95°C for 30 min in a thermocycler. The remaining body of the mosquito was kept in RNAlater individually. From each group, 30 mosquitoes were pooled in sets of 10 females, and RNA was extracted using the Arcturus PicoPure RNA Isolation Kit (Life Technologies). cDNA was synthesized from each RNA pool using Superscript III (Invitrogen) as

previously described (Riveron et al., 2015). The expression pattern of *CYP6P9a* and *CYP6P9b* was assessed by quantitative real-time PCR (qRT-PCR) (Agilent MX3005) to assess the correlation between the presence of the 6.5-kb SV and the expression pattern of these two resistance genes.

2.8 | Assessment of the impact of the 6.5-kb SV on the efficacy of bed nets

2.8.1 | WHO cone bioassays

The efficacy of insecticide-treated net against the strains used was tested using a cone assay following the WHO protocol (WHO, 2013). Mosquitoes from the F_6 generation of the FUM0Z-R and FANG crosses were tested against two WHO recommended LLINs (PermaNet 2.0 and PermaNet 3.0). PermaNet 2.0 nets consist of polyester coated with the deltamethrin to a target dose of 55 mg/m² (\pm 25%) while PermaNet 3.0 has a higher dose of deltamethrin of 85 mg/m² (\pm 25%) and piperonyl butoxide (PBO), a synergist incorporated with deltamethrin in the polyethylene roof (Vestergaard, Frandsen). Briefly, five replicates of 10 F_6 females (2–5 days old) were placed in plastic cones attached to 30 \times 30-cm pieces of nets PermaNet 2.0, PermaNet 3.0 (side) and PermaNet 3.0 (roof), and an insecticide-free net as a control. After 3 min of exposure, the mosquitoes were transferred in holding paper cups and provided with cotton soaked in a 10% sugar solution. Mortality was recorded 24 hr after exposure. The bed nets were tested against the susceptible Kisumu laboratory strain before using them for the study.

2.8.2 | Experimental hut trials

To assess the association between the 6.5-kb SV and a potential reduction in the efficacy of insecticide-treated nets, an experimental hut trial was performed in a field station (possessing 12 huts) located at Mibellon (6°4'60"N, 11°30'0"E), a village in Cameroon located in the Adamawa Region (Mayo Banyo division and Bankim Sub-division). A release recapture experiment was done using F_5 and F_6 generations of the FANG/FUM0Z-R crosses where about 50–100 female mosquitoes were released in each hut at 8:00 p.m. with a volunteer sleeping under each net (PermaNet 2.0, PermaNet 3.0 and control with no insecticide). All the windows of each hut were closed from outside to prevent entry of free flying mosquitoes. The 45° oblique shape of the window openings also does not allow mosquitoes to escape, in addition to the windows being completely closed from outside. Both alive and dead, blood-fed and unfed mosquitoes were collected in the morning. This involved three treatments: the first was untreated polyethylene net, the second PermaNet 2.0 (impregnated with deltamethrin), and the last PermaNet 3.0 (impregnated with PBO and deltamethrin). Six holes of 4 \times 4 cm were made on each net following WHO guidelines to simulate a worn net. Volunteers were recruited from the village to sleep under the nets

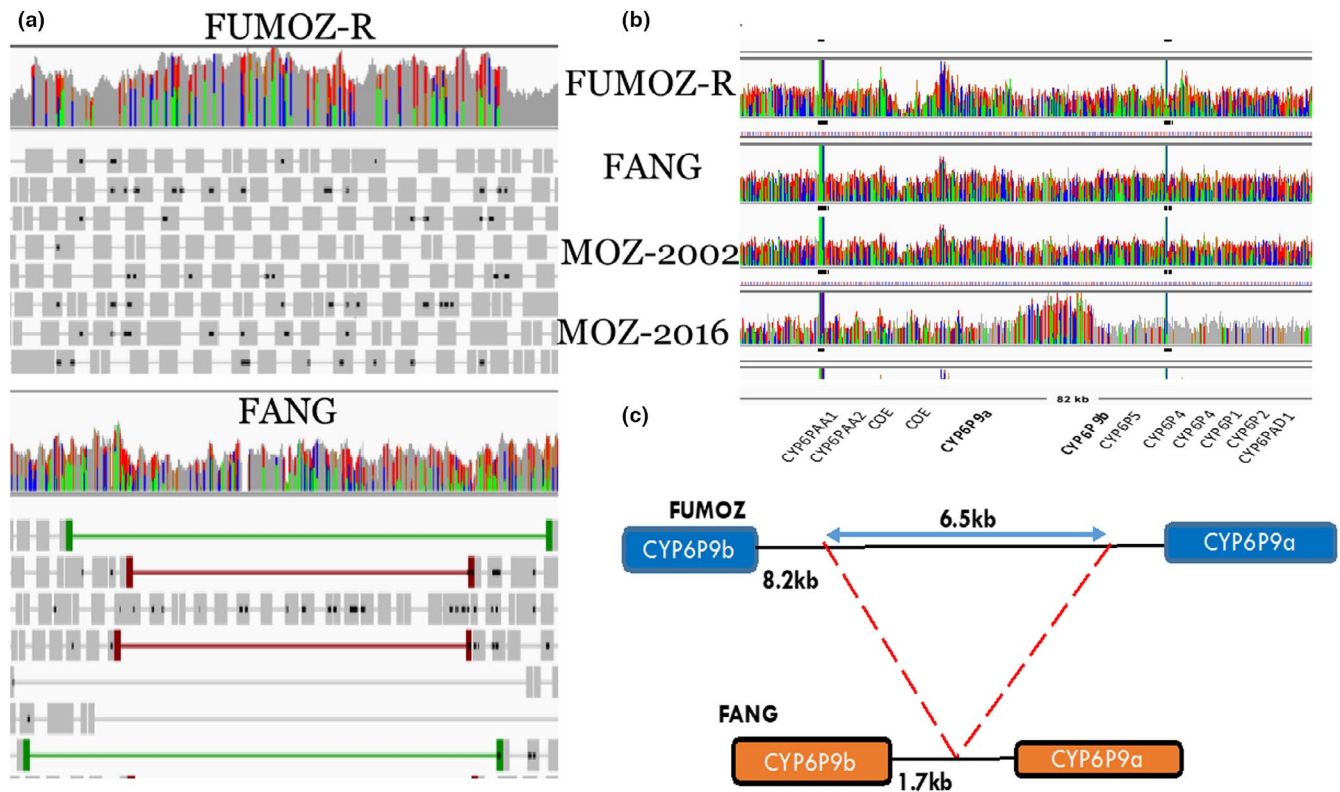


FIGURE 1 Detection of the 6.5-kb intergenic insertion between *CYP6P9a* and *CYP6P9b* in *Anopheles funestus* mosquitoes. (a) Screenshot from the integrative genomics viewer (IGV), showing the coverage depth and aligned reads for the pyrethroid-resistant FUMOS-R strain (upper) and the fully susceptible FANG (lower) using the pooled template whole genome sequence alignments (Pool-seq). The coverage depth plots show deeper coverage in this region in FUMOS-R but not in FANG. The FANG alignment contains read pairs with unusually long insert sizes, indicated in red in the lower panel (thick lines represent reads, read pairs are linked by thin lines). (b) IGV screenshot showing an increase coverage depth of reads between *CYP6P9a* and *CYP6P9b* in FUMOS-R with a loss of polymorphism (grey) compared to the susceptible FANG strain using Pool-seq data. The same contrast is observed between the 2002 sample from Mozambique before LLIN scale up (MOZ-2002) (high diversity and low coverage of read depth) with the 2016 sample (MOZ-2016) where a greater coverage depth is observed at the intergenic region corresponding to the insertion of the 6.5-kb fragment. (c) Schematic representation of the 6.5-kb insertion in FUMOS-R in comparison to FANG

and collect mosquitoes in the morning. A consent form was obtained from each of the volunteers before participating in the study and participants received chemoprophylaxis during the trial. This study was approved by the National Ethics Committee of the Ministry of Public Health in Cameroon. Mosquitoes were collected in the morning by each volunteer using tubes. Mosquitoes were collected and carefully grouped according to their location in the hut; that is, if in the main room (the walls, floor and the hut ceiling), inside of each net and the exit traps (veranda). The blood feeding and mortality status of the mosquitoes collected, such as alive/blood-fed, dead/blood-fed, alive/unfed and dead/unfed, were noted.

2.9 | Statistical analysis

Statistical analysis was performed in GraphPad PRISM 7.05 and alpha values for significance were taken at $p < .05$, with all confidence intervals (CI) at 95%. Student's *t*-test was used to compare the means of data obtained for the luciferase assay and qPCR to determine the level of significance. Fisher's exact test was used to determine

whether any difference in proportion observed for the genotype contingency tables is significant and odds ratio was used to quantify the strength of association between the genotype and mortality/blood-feeding status for the data obtained from the cone assay and experimental huts.

3 | RESULTS

3.1 | Delimiting the insertion in laboratory colonies and identifying its presence in different geographical locations in Africa

By aligning the intergenic region between *CYP6P9a* and *CYP6P9b* for FUMOS and FANG, the insertion point was identified at 851 bp from the stop codon of *CYP6P9b* and 840 bp from the start codon of *CYP6P9a*. To determine the geographical extent of the 6.5 kb SV across African populations of *Anopheles funestus*, pooled-template whole-genome sequencing alignments to the 120 kb *rp1* BAC from several locations (Malawi, Ghana, Benin, Cameroon, Uganda,

Mozambique, DRC Kinshasa and DRC Mikalayi) across the range of *A. funestus* were inspected. This *rp1* BAC spans the cytochrome P450 cluster where both *CYP6P9a* and *CYP6P9b* are located (Wondji et al., 2009). Figure 1 shows alignments for FUM0Z-R and FANG, which show both anomalous features. Figure S1 shows the putative left and right ends of the insertion, defined by the presence of “clipped” reads, where the alignment software aligns a part of the read to the reference and “clips” off part of the read that does not align. The FUM0Z-R alignment contains reads that are left-clipped (the leftmost part of the read, as aligned to the reference, is clipped irrespective of the read's orientation: so the 5' end of a read aligned to the positive strand and the 3' end of a read aligned to the negative strand) between BAC sequence positions 37,409 and 37,410 (37,410 being the leftmost base included in the insertion). It also contains reads that are right-clipped between positions 43,954 and 43,955. This defines a region of 6,545 bp. The presence of only left-clipped reads on the left of the region and right-clipped reads on the right of the region indicates two things in FUM0Z-R: (a) that the “insertion” form of the indel is fixed in the FUM0Z-R sample (there is no evidence for the presence of the “deletion” form), and (b) that the inserted sequence is homologous to part of a larger sequence found elsewhere in the genome (indicated by the “clipped” parts of the reads). In the susceptible FANG, the situation is more complicated. At the left end of the insertion, there are reads left-clipped between positions 37,409 and 37,410 (as for FUM0Z-R) but also some reads right-clipped slightly further left, between positions 37,404 and 37,405. At the right end of the insertion, there are reads right-clipped between positions 43,954 and 43,955 (as for FUM0Z-R) but also some reads left-clipped between the same positions. Also, further to the right there are some reads right-clipped between positions 44,053 and 44,054 and some left-clipped between positions 44,070 and 44,071. Detailed inspection of the clipped reads showed that the reads right-clipped at 37,404/37,405 and left-clipped at 43,954/43,955 indicate the “deletion” form of the indel, as the clipped parts of the reads from the left and right end of the insertion overlap each other (but also contain a short length of DNA that does not match FUM0Z-R). The clipping at 44,053/44,054 and 44,070/44,071 is due to a region of 35 bp in FANG (TAATACGGGAGATACATGGAGCTCGTGTAAGA) that does not align with the FUM0Z reference (ATATGTCGGAGGTTTAT) at the same location. Overall, FANG shows evidence of the “deletion” form of the indel in addition to the presence of the large homologous sequence elsewhere in the genome (Figure 1a). This makes simple inspection of the alignment misleading, as rather than a loss of coverage across the 6.5-kb indel, coverage is seen due to reads originating from sequence elsewhere in the genome. This is illustrated in Figure S1A. Overall, FUM0Z-R exhibits an increased coverage depth of reads between *CYP6P9a* and *CYP6P9b* with a loss of polymorphism compared to the susceptible FANG strain (Figure 1b). The same contrast is observed between the 2002 sample from Mozambique before the scale-up of LLIN (2002) with low coverage of read depth in contrast to the 2016 sample showing a greater coverage depth at the intergenic region corresponding to the insertion of the 6.5-kb fragment.

The results also indicate that the 6.5-kb insertion between *CYP6P9a* and *CYP6P9b* was present only in the southern African population of Malawi, where it was nearly fixed (only a single read in Malawi supported the deletion haplotype) (Table S1). However, populations from other parts of Africa showed no evidence of the insertion haplotype.

Evidence that the insertion probably existed (albeit at low frequency) in the early 2000s comes from its presence in the FUM0Z-R colony, which was colonized from the field in Mozambique in 2000, and subsequently selected for insecticide resistance, which appears to have fixed the insertion haplotype in the colony. However, one could not also rule out a de novo occurrence of this SV in FUM0Z-R during the selection process.

3.1.1 | Investigating the genomic origin of the 6.5-kb insertion

To identify the genomic origin of the inserted 6.5-kb sequence, its entire sequence was used to search the *A. funestus* FUM0Z AfunF3 reference genome assembly using BLASTN implemented in the VectorBase web resource. The results indicated that the sequence occurred at another different location in the genome, on scaffold CM012071.1 (Figure S2A). That location is between 8,296,288 and 8,555,956, ~260 kb away from the *CYP6* cluster on the same scaffold (therefore, on the same chromosome 2). Both loci are on chromosome 2R in the same genomic region as the P450s cluster *rp1* quantitative trait locus (Wondji et al., 2009) which confers high pyrethroid resistance and shown to have undergone a major selective sweep. In addition, short (100 bp) sequences from the left and right ends of the insertion were used to conduct BLASTN searches of AfunF3 and confirmed the results obtained with the full-length insertion sequence. Finally, clipped sequences from immediately to the left and right of the insertion were used to conduct BLASTN searches of AfunF3. The results (matches only adjacent to the CM012071.1:8,296,288–8,555,956 region) confirmed that the “parent” sequence of the insertion between *CYP6P9a* and *CYP6P9b* came from CM012071.1:8,296,288–8,555,956. This putative genomic “parent” sequence of the insert contains no annotated protein-coding genes but there is a large assembly gap in the region. The orthologous region in the *Anopheles gambiae* genome is also on chromosome arm 2R (Figure S2B). The protein-coding genes flanking the insertion sequence, AFUN008344 and AFUN008346, are orthologous to AGAP002842 and AGAP002845, respectively. *A. gambiae* also has no annotated protein-coding genes between AGAP002842 and AGAP002845, suggesting that *A. funestus* may not have also. Two micro-RNAs annotated in both species are outside of the insertion sequence. Despite the lack of annotated genes, the region is transcribed as supported by FUM0Z-R RNA sequencing showing a large transcribed region (Figure S2C), with some evidence of splicing, covering the two annotated micro-RNAs. Whether this transcript is processed to form mature micro-RNAs is not known.

3.2 | Comparative promoter analysis of the *CYP6P9a*–*CYP6P9b* intergenic region

The location of the 6.5-kb insertion in the intergenic region between *CYP6P9a* and *CYP6P9b* (Figure 1c) indicated that this insertion could impact the regulation of these genes. This is strongly supported by their high expression in FUM0Z-R and Southern Africa mosquito populations. To verify this hypothesis, the full-length intergenic fragment (8.2 kb) was successfully PCR-amplified and cloned (Figure S2D) and used for a luciferase reporter assay (Pgl3 FZ6P9a8.2) comparatively with three other construct vectors without the 6.5-kb SV (Pgl3 FZ6P9a0.8, Pgl3 FG6P9a0.8 and Pgl3 LRIM). These constructs were transfected alongside Renilla luciferase plasmid in the *A. gambiae* 4a-2 cell line. The samples were lysed and luciferase activity was measured and normalized against Renilla activity. The luciferase activity of the construct with the 6.5-kb SV from FUM0Z-R, Pgl3

FZ6P9a8.2, was five-fold significantly higher ($p = .00012$) than that of the same strain without it, FZ6P9a0.8, and 17.5-fold higher than the FANG fragment, Pgl3 FG6P9a0.8 ($p < .0001$). This result implies that this insertion probably contains *cis*-regulatory elements acting as gene regulation enhancers and driving the high expression of *CYP6P9a* and *CYP6P9b* observed (Figure 2a).

3.3 | A simple PCR assay to detect the 6.5-kb SV and associated pyrethroid resistance

The 8.2-kb (SV+) and 1.7 kb (SV-) intergenic regions were used to design a simple PCR assay capable of detecting the 6.5-kb structural variant. The PCR comprised three primers, two in the flanking region and one in the 6.5-kb region (Figure 2b). The presence of the SV is shown by the amplification of a fragment of 596-bp (SV+) whereas the

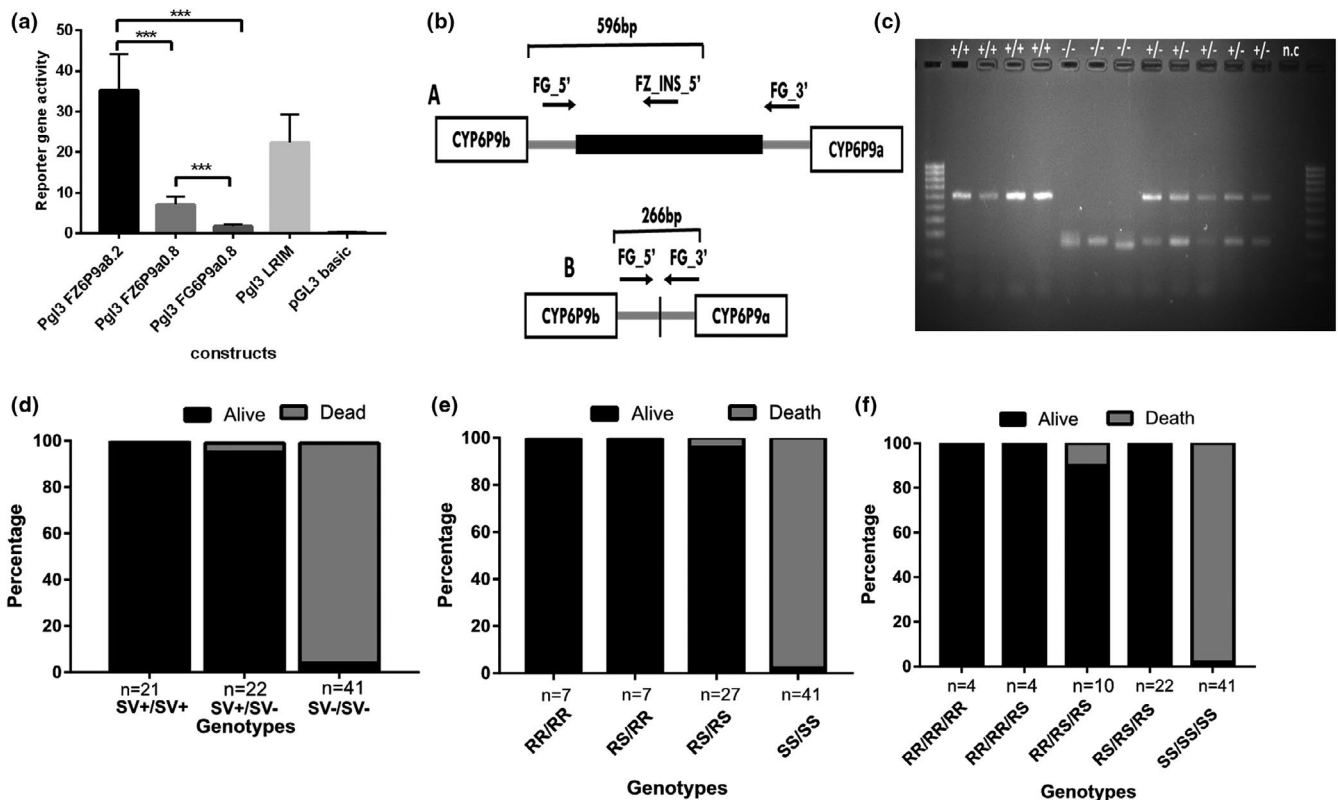


FIGURE 2 Functional characterization of the 6.5-kb SV and design of a PCR diagnostic assay. (a) Comparative Luciferase reporter assay (normalized to renilla fluorescence) of various intergenic fragments between *CYP6P9a* and *CYP6P9b*. Pgl3 FZ6P9a8.2 is the fragment for the full 8.2 intergenic region containing the 6.5-kb insertion showing a highly elevated activity compared to others. Pgl3 FZ6P9a0.8 is the 800 bp region upstream of *CYP6P9a* containing *cis*-regulatory elements used to design the PCR assay for *CYP6P9a* (Weedall et al., 2019) whereas Pgl3 FG6P9a0.8 is the FANG version. Bars represent the mean \pm SD of five independent transfections of three replicates ($n = 5$). (b) Schematic representation of the design of the PCR assay to detect the 6.5-kb insertion using three primers, two located immediately outside of the SV (FG_5' and FG_3'; size of 266 bp if no SV) and one located within the 6.5-kb SV, allowing us to detect its presence (expected band 596 bp). (c) Agarose gel showing the three genotypes indicating the presence (+) or absence (-) of the insertion using F₈ FUM0Z \times FANG crosses. Ladder: 100 bp, n.c.: negative control. (d) Distribution of the 6.5-kb SV genotypes between susceptible (Dead) and resistant (Alive) mosquitoes after WHO bioassays with 0.75% permethrin showing a very strong correlation between the 6.5-kb SV and pyrethroid resistance phenotype. (e) Distribution of the combined genotypes of 6.5 kb and that of *CYP6P9a* after WHO bioassays with 0.75% permethrin showing that both genotypes combined to increase pyrethroid resistance. (f) Distribution of the combined triple genotypes of 6.5 kb besides that of both P450s *CYP6P9a* and *CYP6P9b* after WHO bioassays with 0.75% permethrin, showing that the triple genotypes combined to further increase pyrethroid resistance

absence is shown by a band at 266 bp (SV⁻) (Figure 2c). To assess the efficacy of this novel PCR, we genotyped the FANG-S and FUMOS-R strains for the 6.5-kb SV and found that all FUMOS-R mosquitoes genotyped were homozygous for insertion (SV⁺/SV⁺) while all the FANG mosquitoes were homozygous without insertion (SV⁻/SV⁻).

To assess the association between this 6.5-kb SV and pyrethroid resistance in *A. funestus*, F₈ mosquitoes obtained from crossing FANG and FUMOS-R which had been exposed to 0.75% permethrin for 180 min to get highly resistant (alive) mosquitoes and 30 min to get highly susceptible (dead) mosquitoes were genotyped for this SV. Genetic crosses between FANG and FUMOS-R were used to reduce the bias due to the background of the strains. The results revealed that those alive after 180 min of exposure were mainly homozygous (21/45) and heterozygous (22/45) for the 6.5-kb SV. Only 2/45 alive were lacking the 6.5-kb SV. Genotyping of the 41 highly susceptible mosquitoes revealed that 40/41 were homozygous without the 6.5-kb SV and 1/41 heterozygous (Figure 2d). Consequently, a strong association was found between permethrin resistance and 6.5-kb SV genotype with a highly significant odds ratio (OR) when comparing the homozygote (SV⁺/SV⁺) to the homozygote (SV⁻/SV⁻) (SS) (OR = 2079.4, $p < .001$, Fischer's exact test). Similarly, a significantly higher ability to survive was observed for the heterozygote (SV⁺/SV⁻) when compared to the homozygote (SV⁻/SV⁻) (OR = 600.25, $p < .001$, Fischer's exact test) (Figure 2d) (Table S2). Moreover, analysis of the combined effect of the 6.5-kb SV with the two nearby P450s revealed increased survivorship when the 6.5-kb SV is combined to either *CYP6P9a* (Figure 2e; Table S2) or *CYP6P9b* (Table S2) with an even greater chance to survive when a mosquito is triple homozygous for the resistant allele at the three loci (Figure 2f; Table S2).

3.4 | Enhancer's effect of the 6.5-kb SV on the expression of nearby genes

To confirm the potential enhancer role of the 6.5-kb SV on the regulation of nearby P450 genes, as suggested by the luciferase promoter assay, qRT-PCR was used to compare the expression of the nearby *CYP6P9a* and *CYP6P9b* P450 genes. Mosquitoes obtained from F₂ crossing of FUMOS-R and FANG were pooled into three groups based on their genotypes (SV⁺/SV⁺, SV⁺/SV⁻ and SV⁻/SV⁻) for the 6.5-kb SV (Figure 3a,b). The analysis revealed that the mosquitoes possessing the 6.5-kb SV (SV⁺/SV⁺ and SV⁺/SV⁻) had a significantly higher expression level for *CYP6P9a* and *CYP6P9b* as opposed to those without the 6.5-kb SV (SV⁻/SV⁻) (Figure 3c). The expression level of *CYP6P9a* for mosquitoes with the SV⁺/SV⁺ genotype was about 1.7-fold ($p = .03$) higher than that of SV⁺/SV⁻ genotype and 5.2-fold higher than the homozygote without SV (SV⁻/SV⁻) ($p = .005$). A similar pattern was observed for *CYP6P9b* with the homozygote SV⁺/SV⁺ genotype expressing *CYP6P9b* about two-fold higher than heterozygote mosquitoes ($p = .003$) and 4-fold higher than the homozygote SV⁻/SV⁻ ($p = .001$). This suggests a strong association between the 6.5-kb SV and increased expression

of *CYP6P9a* and *CYP6P9b* probably as a result of the presence of cis-regulatory elements in the 6.5kb acting as enhancers.

3.5 | Geographical distribution of 6.5-kb SV across Africa

This novel diagnostic PCR was tested on wild-collected *A. funestus* mosquitoes from various African regions to determine the spread of this insertion across the continent. Genotyping of the 6.5-kb SV was successful in all the seven countries, revealing that this SV is present in Southern Africa mosquito populations but absent from those collected in Central and Western Africa (Figure 4a). The frequency of 6.5-kb SV was very high in southern Africa ranging from 82% in Zambia (collected in 2015), 92% in Malawi (2014), and 100% in Mozambique (2016) (Figure 4b). Tanzania (2015) and Eastern Democratic Republic of Congo (2015) presented intermediate frequencies (43.94% and 72.2%, respectively). The 6.5-kb SV was completely absent in Western (Ghana, 2014), Eastern (Kenya [2014], Uganda [2014]), and Central Africa (Cameroon [2016] and DRC-Kinshasa [2015]). Hence this SV is confined to Southern Africa as with the *CYP6P9a* and *CYP6P9b* P450-based pyrethroid resistance (Mugenzi et al., 2019; Weedall et al., 2019) and contrary to the L119F and A296S resistance-to-dieldrin (RDL) mutation, which confers DDT and dieldrin resistance respectively (Riveron et al., 2014). Samples from Tanzania and DRC-Mikalayi that show segregation of different genotypes were further used to assess the potential association between the 6.5-kb SV, *CYP6P9a* and *b* (Figure 4c; Figure S3A,B). In Tanzania, a greater linkage of the three markers was observed with 54.8% (17/31) identical genotypes detected while the value was lower in DRC-Mikalayi at 32% (8/25). Considering only *CYP6P9a* and the 6.5-kb SV, 12% (3/25) and 16% (5/31) had the same genotype for both markers for DRC-Mikalayi and Tanzania respectively. A low genotypic frequency of 8% (2/25) was obtained for samples with the same genotype for *CYP6P9b* and the 6.5-kb SV for DRC-Mikalayi. Concerning *CYP6P9a* and *CYP6P9b*, 48% (12/25) and 25.81% (8/31) from DRC-Mikalayi and Tanzania respectively had the same genotype (Figure 4c).

3.6 | The 6.5-kb SV is associated with reduced bed net efficacy

The association between the 6.5-kb SV and bed net efficacy was assessed using mosquitoes previously used to validate *CYP6P9a* (Weedall et al., 2019) and *CYP6P9b* (Mugenzi et al., 2019). Mosquitoes from the FUMOS and FANG crossings were reared to the F₆ generation, which was used for cone assays and to perform a release recapture in experimental huts.

3.6.1 | Cone assays

To validate the ability of the 6.5-kb SV marker to predict the impact of resistance on the efficacy of LLINs, we genotyped F₆ samples

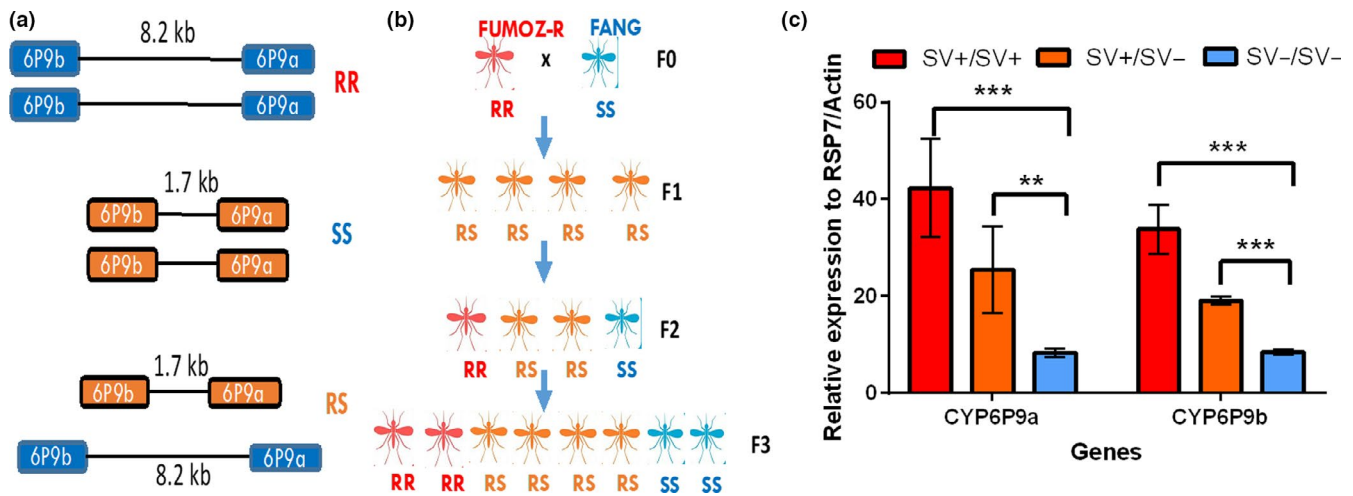


FIGURE 3 Investigation of the enhancer role of the 6.5-kb SV using comparative gene expression profile of the three SV genotypes on *CYP6P9a* and *CYP6P9b*. (a) Schematic representation of the three 6.5-kb SV genotypes expected in *Anopheles funestus* mosquitoes during the crossing process. (b) Experimental design of the crossing between the pyrethroid-resistant strain FUMOS-R (with 100% SV) and the fully susceptible FANG (no SV) up to the F₃ generation. Expected segregation of genotypes is shown. (c) Differential qRT-PCR expression for different insertion genotypes of two cytochrome P450 genes in the immediate vicinity of the 6.5-kb SV. Error bars represent standard deviation ($n = 3$)

obtained from cone assays with PermaNet 2.0 and PermaNet 3.0 (side). A mortality rate of 100% was obtained when the Kisumu susceptible strain was exposed to these nets. Mortality rates were 31.1% and 40.7% for PermaNet 2.0 and PermaNet 3.0 respectively with no significant difference ($p = .380$). With PermaNet 2.0, a significant difference in the distribution of genotypes of the SV was observed between dead and alive mosquitoes ($\chi^2 = 892$; $p < .0001$, Chi-square test) (Figure 5a). Comparing the proportion of each SV genotype between alive and dead mosquitoes revealed that SV+/SV+ homozygote mosquitoes were significantly more likely to survive exposure to PermaNet 2.0 than those completely lacking the SV (SV-/SV-) (OR = 1,798.3; CI = 97.6–33,141; $p < .0001$, Fisher's exact test). Heterozygotes were also more able to survive exposure to PermaNet 2.0 than homozygotes lacking the SV (SV-/SV-) (OR = 261.5; CI = 15.4–4,447.3; $p < .0001$, Fisher's exact test). SV+/SV+ homozygous mosquitoes were also more able to survive than heterozygotes (OR = 7.4; CI = 2.5–21.5; $p = .0002$, Fisher's exact test) showing an additive effect of the 6.5-kb SV on the resistance phenotype. When comparing at the allelic level, it was observed that possessing a single SV+ allele provides a significant ability to survive exposure to PermaNet 2.0 compared to the SV- allele (OR = 27.7; CI = 12.9–59.0; $p < .0001$, Fisher's exact test) (Figure 5a; Table S3). A similar trend was observed with PermaNet 3.0 (side) (Figure 5a; Table S4) whereas we could not assess PermaNet 3.0 (Top) as there were no survivors after exposure.

3.6.2 | Experimental hut trial

Different sets of mosquitoes were released over four consecutive nights in a release-recapture experiment and used to validate the

influence of the 6.5-kb SV on bed net efficacy. Mortality rates were 98.7% for PermaNet 3.0 and 33.3% for PermaNet 2.0 (Weedall et al., 2019). To avoid bias due to exophily and feeding status, only samples that were unfed and in the room were used. A significant difference was observed in the distribution of genotypes of the SV among the alive and dead mosquitoes ($\chi^2 = 40.2$; $p < .0001$, Chi-square test) (Figure 5b,c). Comparison of the proportion of different genotypes among the dead and alive mosquitoes revealed that 6.5-kb SV homozygotes (SV+/SV+) were able to significantly survive exposure to PermaNet 2.0 more than those without the 6.5-kb SV (SV-/SV-) (OR = 27.7; CI: 13.0–59.0; $p < .0001$, Fisher's exact test; Table 1). Mosquitoes heterozygous for the 6.5-kb SV (SV+/SV-) also survived exposure to PermaNet 2.0 more than homozygotes without the 6.5-kb SV (SS) (OR = 7.5; CI: 3.8–14.8; $p < .0001$, Fisher's exact test). However, the 6.5-kb SV heterozygotes (SV+/SV-) survived less than the 6.5-kb SV homozygotes (SV+/SV+) (OR = 3.7; CI = 1.9–7.1; $p = .0001$, Fisher's exact test), suggesting that there is an additive effect associated with possessing two copies rather than one. This was further demonstrated by the ability of mosquitoes having a single 6.5-kb SV to survive more than those without (Figure 5b). A similar trend was observed when the analysis was performed without excluding exophilic status and blood-fed status (Table S5) as well as for PermaNet 3.0 (Figure S4A, Tables S6 and S7).

The distribution of the 6.5-kb SV in blood-fed mosquitoes was assessed to determine any association between this SV and the ability of mosquitoes to blood-feed in the presence of the bed-net. A greater number of mosquitoes were able to blood-feed with PermaNet 2.0 (14.8%) compared to PermaNet 3.0 (6.8%) (Weedall et al., 2019). A significant difference was observed for the distribution of the 6.5-kb SV genotypes between blood-fed and unfed mosquitoes collected from huts with both PermaNet

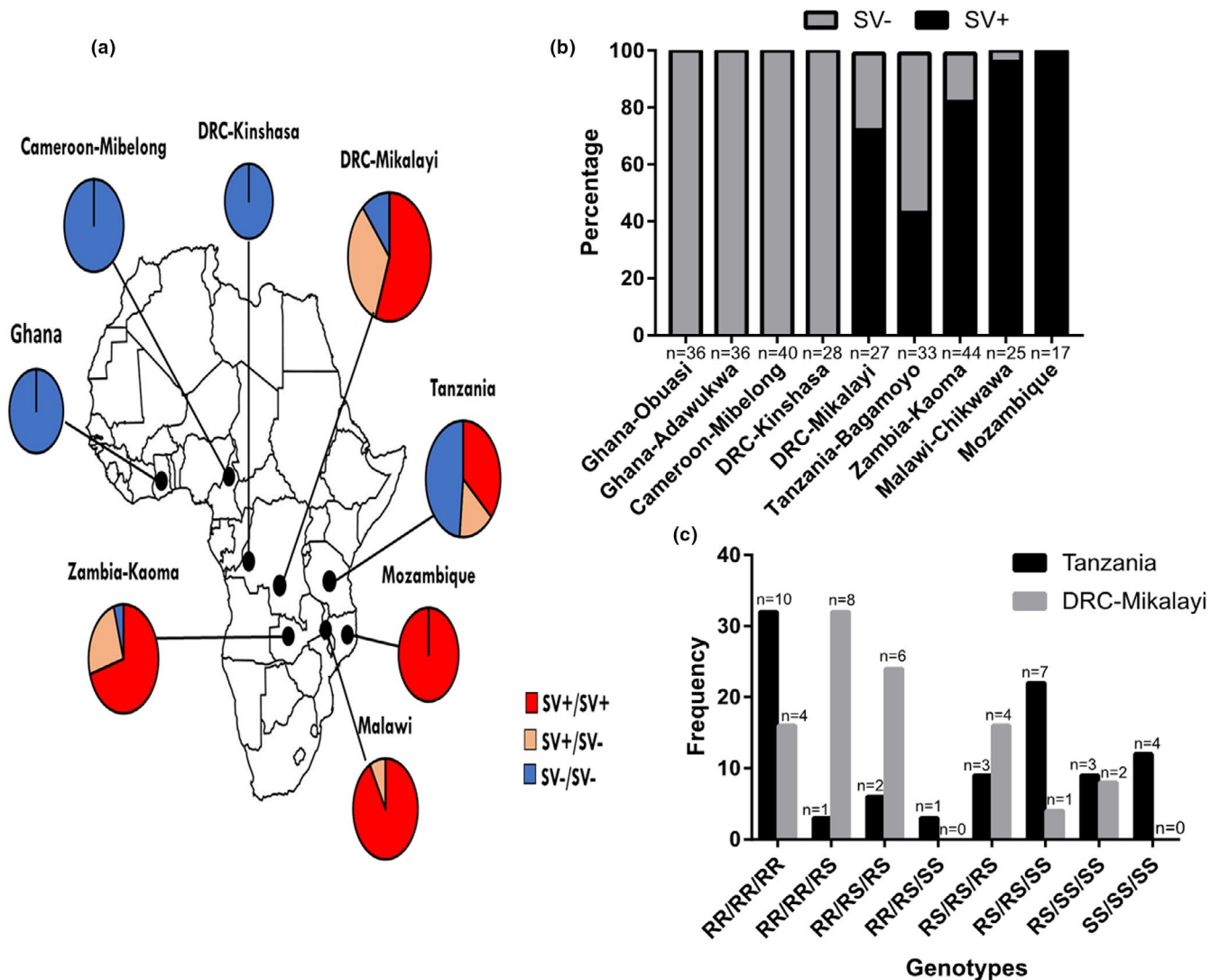


FIGURE 4 Geographical distribution of the 6.5-kb SV across Africa. (a) Map of Africa showing the genotypic distribution of the 6.5-kb SV across the continent which correlated with the CYP6P9a_R and CYP6P9b_R allele distribution. (b) Histogram showing the frequency of the SV+ and SV- alleles across Africa, revealing a clear gradient from Mozambique (100% SV+) to West/Central Africa (0% SV+). (c) Distribution of the combined genotypes CYP6P9a, CYP6P9b and 6.5kb SV in Tanzania and DRC Mikalayi showing extensive segregation of the genotypes to these loci in the field

3.0 ($\chi^2 = 18.4$; $p < .0001$) and PermaNet 2.0 ($\chi^2 = 60.2$; $p < .0001$). A significant association was observed between the 6.5-kb SV genotypes and the ability of mosquitoes to blood-feed when exposed to PermaNet 3.0. Mosquitoes homozygous for the 6.5-kb SV (SV+/SV+) were more likely to blood-feed in the presence of PermaNet 3.0 than those homozygous without (SV-/SV-) (OR = 355.2; CI = 21.4–5,889.4; $p < .0001$) and heterozygous for the 6.5-kb SV (SV+/SV-) (OR = 2.6; CI = 1.3–4.0; $p = .00489$). Mosquitoes heterozygous for the 6.5-kb SV (SV+/SV-) were also able to blood-feed more than those without the SV (SV-/SV-) (OR = 158.3; CI = 9.6–2,620.0; $p = .0004$) (Figure 5d; Table 2). Analysis of genotype distribution for PermaNet 2.0 gave similar trends, but these were not significant apart from SV+/SV- vs. SV-/SV- (Figure S4B, Table S8).

3.7 | The 6.5-kb SV combines with CYP6P9a and CYP6P9b to further reduce LLIN efficacy

We next assessed the impact of different combinations of genotypes for the three loci on the efficacy of LLINs. The cone assay results revealed increased survivorship when the 6.5-kb SV was combined with CYP6P9a for PermaNet 2.0 (Figure S5A; Table S3) and PermaNet 3.0 (side) (Figure S5B; Table S4). Similar patterns were observed when combined with CYP6P9b (Figure S5C,D; Tables S3 and S4). Mosquitoes triple homozygous for the resistant allele at the three loci exhibited a greater ability to survive than all other genotype combinations for both nets (Figure S5E,F; Tables S3 and S4).

Experimental hut trials also showed that triple RR/RR/SV+/SV+ homozygotes were more likely to survive exposure to PermaNet

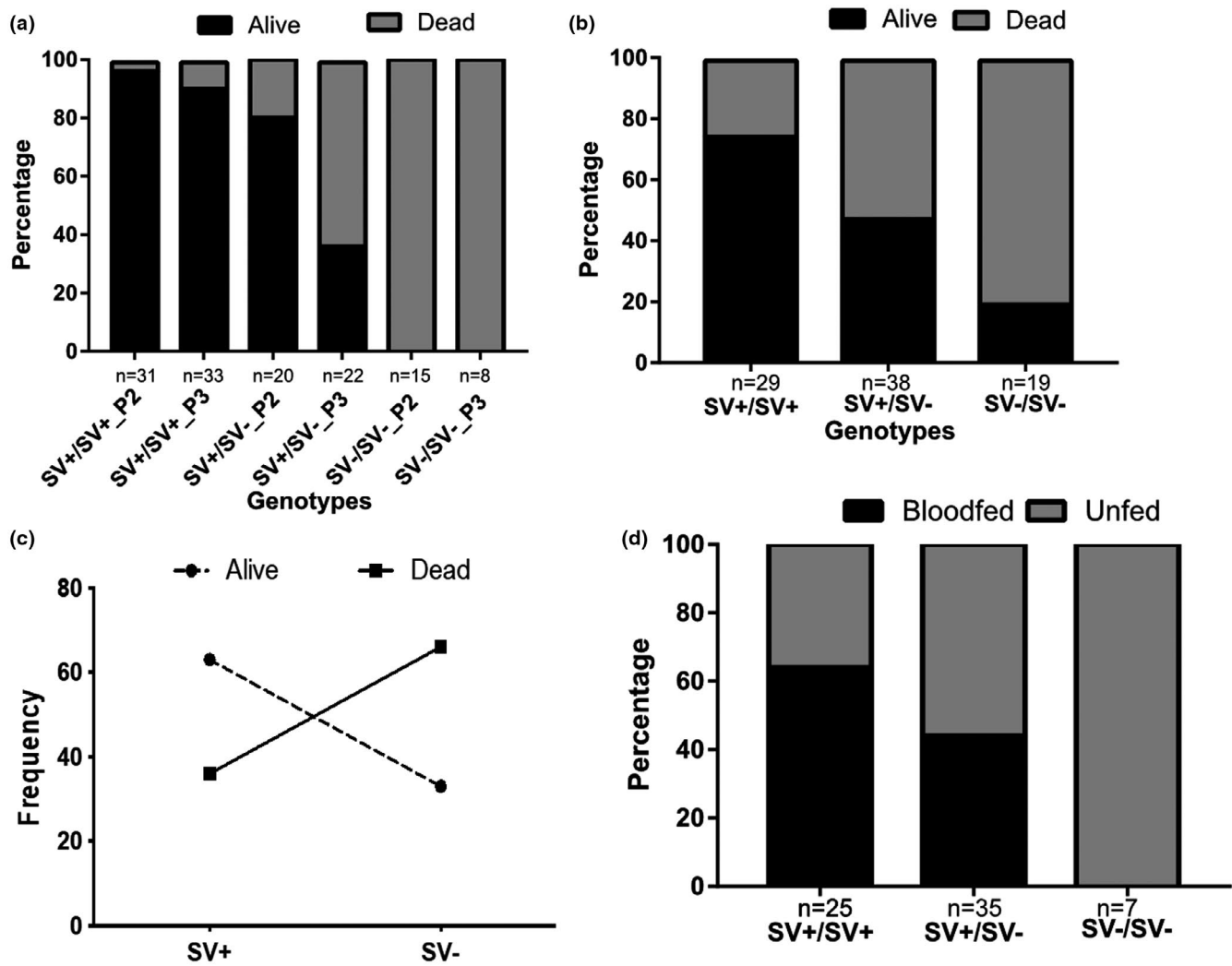


FIGURE 5 Impact of the 6.5-kb enhancer on the efficacy of insecticide-treated nets using experimental hut trials. (a) Distribution of 6.5-kb SV genotypes among mosquitoes that survive exposure to PermaNet 2.0 (P2) and PermaNet 3.0 (side) (P3) and those that died using cone assays, showing an increased ability to withstand exposure to bed nets when possessing one and two copies of the 6.5-kb SV. (b) Distribution of 6.5-kb SV genotypes between dead and alive mosquitoes after exposure to PermaNet 2.0 net in huts, showing that the 6.5-kb SV significantly allows mosquitoes to survive exposure to this bed net. (c) Correlation between the frequency of 6.5-kb SV alleles and ability to survive exposure to PermaNet 2.0 Odds ratio = 3.5; 95% CI: 1.9486–6.2866 and $p < .0001$. (d) Distribution of the 6.5-kb SV genotypes between blood-fed and unfed mosquitoes after exposure to the PBO-based net PermaNet 3.0 in huts, showing that the SV+ allele increases the ability to take a blood meal even for PBO-based nets

2.0 than any other combined genotype (Figure 6a; Table 1). RR/RR/SV+/SV+ survived more than the SS/SS/SV-/SV- (OR = 2,505.8; CI: 141.1–44,486.7; $p < .0001$), RR/RS/SV+/SV- (OR = 31.0; CI = 1.8–529.3; $p = .0177$) and RS/RS/SV+/SV- mosquitoes (OR = 134.6; CI: 8.1–2228.4; $p = .0006$). There was no significant difference between the RR/RR/SV+/SV+ and RR/RR/SV+/SV- genotypes (OR = 1; CI = 0.02–50.9; $p = 1.0$) and both had a similar trend in terms of survival with the same odds ratio (Figure 6b; Table 1). Hence, there is an additive advantage associated with the mosquito combined genotype at the three loci which confers a higher level of pyrethroid resistance and leading to a greater reduction in bed net efficacy. The impact decreased in the order RR/RR/SV+/SV+ = RR/RR/SV+/SV- > RR/RS/SV+/SV- > RS/RS/SV+/SV- > SS/SS/SV-/SV-. This additive effect

was also observed for the PBO-based PermaNet 3.0 net although to a lower extent (OR = 423; $p < .0001$; RRR/RR/SV+/SV+ vs. SS/SS/SV-/SV-) (Figure S4C; Tables S6 and S7). Moreover, an increased ability to survive exposure to LLIN was observed even when combining genotypes of the 6.5-kb SV only to either of CYP6P9a (Figure S6A,B) or CYP6P9b (Figure S7A,B).

In addition to the ability to survive bed net exposure, RR/RR/SV+/SV+ also had a higher ability to blood-feed compared to SS/SS/SV-/SV- (OR = 5.0; CI: 2.7–9.0; $p < .0001$) and the other combinations in the presence of PermaNet 3.0 (Figure 6c,d). This additive effect was also observed when combining genotypes of the 6.5-kb SV only to either of CYP6P9a (Figure S6C,D) or CYP6P9b (Figure S7C,D). For PermaNet 2.0 no significant association was observed (Figure S4D; Table S8).

TABLE 1 Correlation between genotypes of the 6.5-kb SV and ability to survive exposure to PermaNet 2.0 in experimental huts using unfed samples

Genotype comparison	Odds ratio (OR)	Confidence interval (CI)	p value
6.5 SV			
SV+/SV+ vs. SV-/SV-	27.7	13.0–59.0	<.0001
SV+/SV+ vs. SV+/SV-	3.7	1.9–7.1	.0001
SV+/SV- vs. SV-/SV-	7.5	3.8–14.8	<.0001
SV+ vs. SV-	5.8	3.1–10.7	<.0001
CYP6P9a/SV			
RR/SV+SV+ vs. SS/SV-SV-	17.2	7.8–38.2	<.0001
RS/SV+SV- vs. SS/SV-SV-	8.6	3.9–19.0	<.0001
RR/SV+SV+ vs. RS/SV+SV-	2.0	1.1–3.5	.0163
CYP6P9b/SV			
RR/SV+SV+ vs. SS/SV-SV-	1,936.0	111.1–33,734.8	<.0001
RS/SV+SV- vs. SS/SV-SV-	22.5	10.1–50.4	<.0001
RR/SV+SV+ vs. RS/SV+SV-	91.1	5.5–1,513.9	.0017
CYP6P9a/CYP6P9b/SV			
RR/RR/SV+SV+ vs. SS/SS/SV-SV-	2,505.8	141.1–44,486.7	<.0001
RS/RS/RS vs. SS/SS/SV-SV-	19.9	8.4–47.4	<.0001
RR/RR/RR vs. RS/RS/SV+SV-	134.6	8.1–2,228.4	.0006

TABLE 2 Correlation between genotypes of the 6.5-kb SV and ability to blood-feed when exposed to PermaNet 3.0 in experimental huts

Genotype comparison	Odds ratio (OR)	Confidence interval (CI)	p value
6.5 SV			
SV+/SV+ vs. SV-/SV-	355.2	21.4–5,889.4	<.0001
SV+/SV+ vs. SV+/SV-	2.6	1.3–4.0	.0048
SV+/SV- vs. SV-/SV-	158.3	9.6–2,620.0	.0004
SV+ vs. SV-	2.5	1.4–4.4	.0020
CYP6P9a/SV			
RR/SV+SV+ vs. SS/SV-SV-	4.5	2.5–8.2	<.0001
RS/SV+SV- vs. SS/SV-SV-	2.0	1.1–3.6	.0205
RR/SV+SV+ vs. RS/SV+SV-	2.3	1.3–4.0	.0047
CYP6P9b/SV			
RR/SV+SV+ vs. SS/SV-SV-	4.5	2.5–8.3	<.0001
RS/SV+SV- vs. SS/SV-SV-	2.3	1.3–4.1	.0062
RR/SV+SV+ vs. RS/SV+SV-	2.0	1.1–3.6	.0159
CYP6P9a/CYP6P9b/SV			
RR/RR/SV+SV+ vs. SS/SS/SV-SV-	5.0	2.7–9.0	<.0001
RS/RS/RS vs. SS/SS/SV-SV-	2.1	1.2–3.7	.0141
RR/RR/RR vs. RS/RS/SV+SV-	2.4	1.3–4.3	.0029

3.8 | Scale-up of bed nets is associated with combined selection of 6.5-kb SV, CYP6P9a and CYP6P9b

We assessed how these three loci are being selected for in the field using mosquito samples collected in 2002 and 2016 in southern Africa (Mozambique). The results revealed that the genotypes in the 2002 samples were skewed towards SS/SS/SS (92.59%) while those collected in 2016 were RR/RR/RR (100%) (Figure 6e; and Figure S8). This observed selection of RR/RR/RR marches with the scale-up of bed nets with samples with the RR/RR/RR genotype being completely absent before the introduction of bed nets and its fixation after many years of bed nets usage. Hence scale-up of vector control interventions may have played a major role in the selection of the combined resistant genotype at the three loci.

4 | DISCUSSION

This study investigated the role that SVs in *cis*-regulatory regions play in cytochrome P450-mediated metabolic resistance to pyrethroids in mosquitoes by focusing on a 6.5-kb intergenic insertion

between two duplicated P450s in the malaria vector *Anopheles funestus*. This work showed that the 6.5-kb SV acts an enhancer for nearby duplicated P450 genes CYP6P9a and CYP6P9b, leading to their increased overexpression. This 6.5-kb SV is strongly associated with an aggravation of pyrethroid resistance, which reduces the efficacy of pyrethroid-only nets but also to some extent that of PBO nets. This study improves our understanding of the molecular processes that drive P450-based resistance to insecticides in mosquitoes while providing an additional marker for monitoring pyrethroid resistance in wild *A. funestus* populations.

4.1 | The 6.5kb SV acts as an enhancer for the up-regulation of duplicated P450 genes

The whole-genome Pool-seq confirmation of the 6.5-kb insertion in field populations of *A. funestus* supported the previous report in the laboratory pyrethroid-resistant FUMOS-R strain (Weedall et al., 2019). The present study has shown that this insertion acts as an enhancer to the over-expression of both duplicated P450 genes CYP6P9a and CYP6P9b, which are key pyrethroid resistance genes in

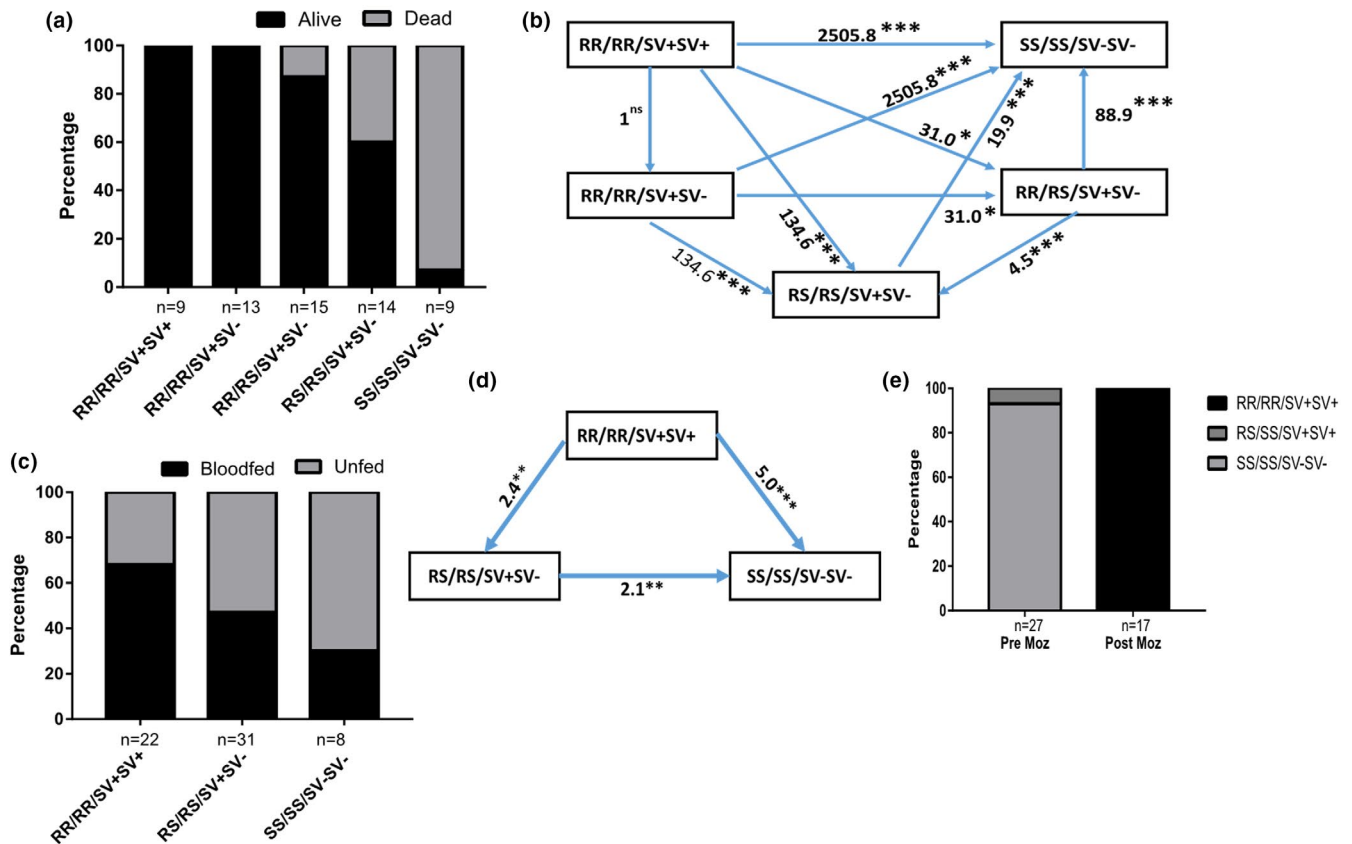


FIGURE 6 The 6.5-kb SV combines with both CYP6P9a_R and CYP6P9b_R P450 alleles to further reduce the efficacy of insecticide-treated nets. (a) Distribution of combined genotypes for CYP6P9a, CYP6P9b and the 6.5-kb SV showing that the three markers combine to increase the chances of being alive in the presence of PermaNet 2.0. (b) Ability to survive exposure to PermaNet 2.0 for the various combined genotypes for the 6.5-kb SV, CYP6P9a and CYP6P9b. * $p < .05$, ** $p < .01$, *** $p < .001$. (c) Distribution of the combined genotypes for the 6.5-kb SV, CYP6P9a and CYP6P9b in mosquitoes collected after exposure to PermaNet 3.0 in huts showing that the three loci combine to increase blood feeding ability. (d) The triple RR/RR/SV+SV+ homozygous mosquitoes for the 6.5-kb SV, CYP6P9a and CYP6P9b exhibit a greater blood feeding ability than other genotypes. (e) Impact of bed net scale-up in Mozambique on selection of the 6.5-kb SV, CYP6P9a and CYP6P9b genotypes with no triple homozygote genotype before (Pre Moz) and 100% after (Post Moz) scale-up of bed nets [Colour figure can be viewed at wileyonlinelibrary.com]

FUMOSZ-R (Amenya et al., 2008; Wondji et al., 2009) and in southern Africa (Riveron et al., 2013; Weedall et al., 2019). The first line of evidence that the 6.5-kb insertion serves as an enhancer was provided by the comparative promoter assays performed between the promoter with the 6.5-kb SV and the core promoter region of CYP6P9a. The greater promoter activity observed in the presence of the SV than in the absence shows that this insertion increases the over-expression of these P450 genes. This is further supported by the previous report that the 6.5-kb SV is highly enriched with regulatory elements, including several transcription factor binding sites as well as several TATA (35), CCAAT (12) and GC (11) sequences. Furthermore, the presence of 51 sites for the Cap n Collar C (CnCC) and the Muscle aponeurosis fibromatosis (Maf) transcription factor sites, which are known xenobiotic sensors in insects (Ingham et al., 2017; Weedall et al., 2019), supports the role probably played by this insertion in enhancing the regulation of neighbouring genes. Analysis of the composition of the 6.5-kb insertion provides good insight into the architectural characteristics of enhancers in mosquitoes and is similar to that of mammals, which have also been

shown to include the multiple transcription factor binding sites as well as transcriptionally activating and repressing domains in the same enhancer (Dickel et al., 2013).

Second, at the transcriptional level, the relative expression of CYP6P9a and CYP6P9b were shown to correlate with the 6.5-kb SV genotypes. The presence of this SV is strongly associated with increased expression of these two genes (SV+/SV+ > SV+/SV- > SV-/SV-), which are located upstream and downstream of this SV. It is well documented that insertions by introducing novel *cis*-acting elements into the regulatory regions can either alter the expression of a gene or disrupt it (Chung et al., 2007). The fact that this 6.5-kb SV is enhancing the expression of two genes is in line with what is already known about enhancers that can regulate genes in the *cis*- position either upstream (e.g., CYP6P9a) or downstream (e.g., CYP6P9b) or even in an intron (Pennacchio et al., 2013). The fact that the presence of the 6.5-kb SV impacts the two genes is also in line with previous reports stating that enhancers can regulate the expression of multiple genes (Pennacchio et al., 2013). It will be good to establish whether this 6.5-kb SV regulates the expression of other

genes besides *CYP6P9a/b*, notably on the cluster of P450s in this *rp1* resistance locus (Wondji et al., 2009).

Third, the geographical distribution of the 6.5-kb SV tightly correlated with the high over-expression of *CYP6P9a* and *CYP6P9b* in the FUMOS-R strain and across southern African countries (Riveron et al., 2013; Weedall et al., 2019) but a low expression elsewhere in Africa where this SV is absent such as in Central, East and West Africa (Riveron et al., 2017). This observation further supports that the 6.5-kb SV is driving the up-regulation of both genes. This is similar to what was reported in *Drosophila melanogaster* where over-expression of the cytochrome P450 gene *Cyp6g1*, conferring DDT resistance, correlated with the insertion of a long terminal repeat (LTR) of an Accord retrotransposon in the regulatory region of this gene (Catania et al., 2004; Daborn et al., 2002). However, contrary to other insertion elements linked to over-expression identified so far, this 6.5-kb insertion does not contain a transposable element but mainly putative *cis*-regulatory elements (Weedall et al., 2019). Nardini et al. (2019) identified transcriptional enhancers in *Anopheles coluzzii* proximal to genes relevant to insecticide resistance (Acetylcholinesterase 1 [ACE1, AGAP001356], GABA-gated chloride channel subunit [Rdl, AGAP006028]) but not in the cytochrome P450 cluster. Future studies can focus on identifying enhancers in the vicinity of genes associated with metabolic resistance in other species such as *A. gambiae* and *Aedes*.

4.2 | Role of the 6.5-kb SV and aggravation of pyrethroid resistance

The design of a simple PCR diagnostic assay to genotype the 6.5-kb SV has allowed us to establish its contribution to the resistance phenotype. First, it has been shown that the 6.5-kb SV segregates independently from *CYP6P9a* and *CYP6P9b* and thus that it is an additional genetic factor driving pyrethroid resistance beside the allelic variation of both genes previously reported (Ibrahim et al., 2015). The independent segregation of the 6.5-kb SV is also shown by the increased pyrethroid resistance that it confers when using either WHO bioassays or cone assays. The fixation of this SV, besides the resistant alleles of *CYP6P9a* and *CYP6P9b*, could explain the resistance escalation currently reported in several mosquito populations of *A. funestus* such as in Mozambique (Riveron et al., 2019) and Malawi (Riveron et al., 2015) and which is reducing the efficacy of insecticide-treated nets (Riveron et al., 2019). The near fixation of the 6.5-kb SV seen in southern Mozambique after bed nets (2016) but its absence before bed net scale up (2002) is an indication that this SV is strongly associated with resistance exacerbation. Fixation of the 6.5-kb SV in highly resistant wild populations also suggests that escalation of pyrethroid resistance could be driven, among others, by an increased metabolic resistance through genetic elements such as enhancers.

The strong association observed between this SV and pyrethroid resistance either with WHO bioassays or with cone assays shows that this SV can be used as a resistance marker for monitoring pyrethroid resistance. This is in addition to the *CYP6P9a* (Weedall

et al., 2019) and *CYP6P9b* (Mugenzi et al., 2019) markers previously identified in the promoters of these genes. This novel assay is even simpler than the PCR-RFLPs previously designed for *CYP6P9a* and *CYP6P9b* as it does not require restriction enzymes. There could be other undetected genetic variations that are also associated with pyrethroid resistance but contributing at different levels.

Detection of this 6.5-kb enhancer in the *cis*-regulatory region of major resistance genes further supports that genetic variations in this region play a major role in driving metabolic resistance, as seen for several resistance genes including the P450 *CYP9M10* in *Culex quinquefasciatus* (Wilding et al., 2012), *GSTe2* in *A. funestus* (Mugenzi et al. submitted) and *CYP6G1* in *Drosophila* (Daborn et al., 2002). Therefore, the *cis*-regulatory region of major metabolic resistance genes should be thoroughly investigated to identify additional markers to design simple DNA-based assays to detect such resistance in mosquitoes.

4.3 | Geographical distribution confirms the restriction of gene flow in *A. funestus*

The geographical distribution of the 6.5-kb SV across Africa mirrors closely that of the resistance alleles of both *CYP6P9a* and *CYP6P9b* P450s (Mugenzi et al., 2019; Weedall et al., 2019) with the highest frequency observed in southern Mozambique (100%) up to eastern DRC (72.2%). It also correlates with the Africa-wide distribution of the N485 Ace-1 carbamate resistance allele in this species (Ibrahim et al., 2016), supporting the existence of an insecticide resistance front in southern Africa which significantly differs from other regions. The south/north clinal increase of frequency in the spread of this SV supports that this resistance probably originated in southern Mozambique and gradually migrated northwards in combination with local selection forces. The absence of the 6.5-kb SV in other regions of Africa is in line with barriers to gene flow between populations in this species across the continent with southern African populations being consistently differentiated from other regions (Barnes, et al., 2017; Barnes, et al., 2017; Michel et al., 2005). Restriction of the 6.5-kb SV to southern Africa can be explained by the presence of different selective pressures across Africa, as recently shown by an Africa-wide study revealing that different regions exhibit different signatures of selective sweep (Weedall et al., 2020). These regional differences could be explained by the fact that local forces driving the development of insecticide resistance may play a greater role than the trans-regional spread of resistance genes due to barriers to gene flow (Weedall et al., 2020). This can lead to different resistance mechanisms in other parts of Africa with different genes associated with insecticide resistance. In contrast, the 6.5-kb SV distribution is opposite to that of other markers in this species, notably the L119F-GSTe2 conferring DDT/pyrethroid resistance (Riveron et al., 2014) and the A296S-RDL dieldrin resistance marker (Wondji et al., 2011). Because the 6.5-kb SV allele was completely absent in 2002 before the scale up of LLINs while

both *CYP6P9a* and *CYP6P9b* were already detectable although at low frequency (10.9% and 5.2%), it is likely that this SV was selected later as the resistance level increased due to greater selection pressure. Analysis of larger temporal samples will further help to track the selection of this SV.

Analysis of the distribution of the 6.5-kb SV and that of *CYP6P9a* and *CYP6P9b* in natural populations revealed that alleles at these markers do segregate independently in the field, as also seen in the hybrid strain FUM0Z-R/FANG at F_4 where most of the genotypic combinations were observed. This suggests that regardless of the proximity of the three loci (a total span of 12 kb), they are not physically linked. The higher linkage frequency observed in Mozambique and Tanzania may be due to stronger insecticide selection applied against these populations as a consequence of the scale-up of vector control interventions (Barnes, et al., 2017). To determine which gene between *CYP6P9a* and *CYP6P9b* is more closely linked to the 6.5-kb SV, the percentage linkage for *CYP6P9a* and the 6.5-kb SV was compared with that for *CYP6P9b* and the 6.5-kb SV in DRC-Mikalayi and Tanzania. For DRC-Mikalayi, *CYP6P9a* and the 6.5-kb SV had more identical genotypes (12%) than for *CYP6P9b* and the 6.5-kb SV (8%), whereas in Tanzania, only *CYP6P9a* and the 6.5-kb SV were identical genotypes (16%) identified and none for *CYP6P9b* and the 6.5-kb SV (0%). Hence, this SV—although impacting both genes as shown by comparative qRT-PCR—appears to have a greater linkage to *CYP6P9a*. This could also support a higher fold-change observed for *CYP6P9a* in the field in southern Africa (Barnes, et al., 2017; Riveron et al., 2013; Weedall et al., 2019). This could be because the 6.5-kb SV is located upstream of the 5' untranslated region (UTR) of *CYP6P9a* but downstream of the 3' UTR of *CYP6P9b*.

4.4 | The 6.5-kb SV aggravates the loss of efficacy of insecticide-treated nets

The design of the simple PCR-based assay to genotype the 6.5-kb SV enabled us to assess the impact of such structural variation on the efficacy of insecticide-treated nets, including the pyrethroid-only and the PBO-synergist nets. The greater reduction of efficacy that the 6.5-kb SV was shown to cause on pyrethroid-only nets than PBO-based nets is similar to that observed with *CYP6P9a* (Weedall et al., 2019) and *CYP6P9b* (Mugenzi et al., 2019) in terms of reduction of mortality rate and blood-feeding inhibition. It further supports the view that PBO-based nets should be deployed to control P450-based metabolically resistant mosquito populations such as *A. funestus* throughout southern Africa. The fact that triple homozygous resistant mosquitoes have a greater ability to survive exposure to LLINs shows that resistance escalation in field populations of vectors is likely to significantly reduce the effectiveness of current pyrethroid-based LLINs. If such resistance escalation involves mechanisms other than just P450s, it could further reduce the efficacy of LLINs, as recently shown for a population of *A. funestus* in southern Mozambique which was even able to survive exposure to some PBO-based nets

(Riveron et al., 2019) due partially to over-expression of *CYP6P9a* and *CYP6P9b* and the fixation of all three resistance alleles (6.5-kb SV, *CYP6P9a*-R and *CYP6P9b*-R) but probably also other mechanisms yet to be elucidated. The availability of additional DNA-based markers such as these will now enable control programmes to assess how resistance is impacting the efficacy of the bed nets in their country and decide whether to adopt PBO-based nets or even new generation nets with classes of insecticide other than just pyrethroids.

In conclusion, by elucidating the role of a 6.5-kb SV in the pyrethroid resistance in *A. funestus*, this study has highlighted the important contribution of SVs in *cis*-regulatory regions in metabolic resistance in mosquitoes. It also highlighted the role of enhancers in the over-expression of metabolic resistance genes. This study designed a simple molecular diagnostic assay to easily monitor this P450-based metabolic resistance in wild populations. The additive resistance confers by this 6.5-kb SV in the presence of *cis*-regulatory promoter factors at *CYP6P9a* and *CYP6P9b* as well as allelic variation in coding regions (Ibrahim et al., 2015) highlights the complex array of evolutionary tools that mosquitoes deploy to survive the scale-up of insecticide-based control interventions such as LLINs. The near fixation of triple resistance (SV/*CYP6P9a*/*CYP6P9b*) in southern Africa calls for urgent action by using insecticides other than pyrethroids for indoor residual spray (IRS) and new generation LLINs with PBO and preferably with a new insecticide class.

ACKNOWLEDGMENTS

The authors thank the inhabitants of Mibellon for their support during the study. This work was supported by Wellcome Trust Senior Research Fellowship in Biomedical Sciences to C.S.W. (101893/Z/13/Z and 217188/Z/19/Z).

CONFLICTS OF INTEREST

The authors declare that they have no competing interests.

AUTHOR CONTRIBUTIONS

C.S.W. conceived the study; C.S.W. and F.C.N. designed the study; G.D.W. and C.S.W. analysed the next-generation sequencing data with assistance from J.H., M.J.W., J.M.R. and M.T., L.M.J.M. and C.S.W. characterized the *CYP6P9a/b* intergenic region and designed the PCR diagnostic assay; L.M.J.M. and M.T. generated the laboratory crosses and performed the validation of the PCR; L.M.J.M. performed the qRT-PCR. B.D.M. performed the experimental hut experiments with C.S.W. and genotyped the 6.5-kb structural variant with M.J.W. and M.T.; C.S.W. and L.M.J.M. wrote the paper with assistance from J.H.; all authors read and approved the final draft of the paper.

DATA AVAILABILITY STATEMENT

All genomic data sets are available from the European Nucleotide Archive. Pooled template whole-genome sequencing data are available under study accessions PRJEB13485 (Malawi 2002 and Malawi 2014), PRJEB24384 (Ghana, Benin, Cameroon and Uganda) and PRJEB35040 (Mozambique 2002, 2016; DRC-Kinshasa and Mikalayli).

ORCID

Leon M. J. Mugenzi  <https://orcid.org/0000-0002-6857-9608>

Jack Hearn  <https://orcid.org/0000-0003-3358-4949>

REFERENCES

- Amenya, D., Naguran, R., Lo, T.-C.-M., Ranson, H., Spillings, B. L., Wood, O. R., Brooke, B. D., Coetzee, M., & Koekemoer, L. L. (2008). Over expression of a cytochrome P450 (CYP6P9) in a major African malaria vector, *Anopheles funestus*, resistant to pyrethroids. *Insect Molecular Biology*, 17(1), 19–25. <https://doi.org/10.1111/j.1365-2583.2008.00776.x>
- Barnes, K. G., Irving, H., Chiumia, M., Mzilahowa, T., Coleman, M., Hemingway, J., & Wondji, C. S. (2017). Restriction to gene flow is associated with changes in the molecular basis of pyrethroid resistance in the malaria vector *Anopheles funestus*. *Proceedings of the National Academy of Sciences of the United States of America*, 114(2), 286–291. <https://doi.org/10.1073/pnas.1615458114>
- Barnes, K. G., Weedall, G. D., Ndula, M., Irving, H., Mzilahowa, T., Hemingway, J., & Wondji, C. S. (2017). Genomic footprints of selective sweeps from metabolic resistance to pyrethroids in African malaria vectors are driven by scale up of insecticide-based vector control. *PLoS Genetics*, 13(2), e1006539. <https://doi.org/10.1371/journal.pgen.1006539>
- Bhatt, S., Weiss, D. J., Cameron, E., Bisanzio, D., Mappin, B., Dalrymple, U., Battle, K., Moyes, C. L., Henry, A., Eckhoff, P. A., Wenger, E. A., Briët, O., Penny, M. A., Smith, T. A., Bennett, A., Yukich, J., Eisele, T. P., Griffin, J. T., Fergus, C. A., ... Gething, P. W. (2015). The effect of malaria control on *Plasmodium falciparum* in Africa between 2000 and 2015. *Nature*, 526(7572), 207–211.
- Catania, F., Kauer, M., Daborn, P., Yen, J., Ffrench-Constant, R., & Schlötterer, C. (2004). World-wide survey of an Accord insertion and its association with DDT resistance in *Drosophila melanogaster*. *Molecular Ecology*, 13(8), 2491–2504. <https://doi.org/10.1111/j.1365-294X.2004.02263.x>
- Chung, H., Bogwitz, M. R., McCart, C., Adrianopoulos, A., Batterham, P., & Daborn, P. J. (2007). Cis-regulatory elements in the Accord retrotransposon result in tissue-specific expression of the *Drosophila melanogaster* insecticide resistance gene Cyp6g1. *Genetics*, 175(3), 1071–1077.
- Daborn, P. J., Yen, J. L., Bogwitz, M. R., Le Goff, G., Feil, E., Jeffers, S., Tijet, N., Perry, T., Heckel, D., Batterham, P., Feyereisen, R., Wilson, T. G., & Ffrench-Constant, R. H. (2002). A single P450 allele associated with insecticide resistance in *Drosophila*. *Science*, 297(5590), 2253–2256.
- Dickel, D. E., Visel, A., & Pennacchio, L. A. (2013). Functional anatomy of distant-acting mammalian enhancers. *Philosophical Transactions of the Royal Society of London. Series B, Biological Sciences*, 368(1620), 20120359. <https://doi.org/10.1098/rstb.2012.0359>
- Hall, T. A. (1999). *BioEdit: A user-friendly biological sequence alignment editor and analysis program for Windows 95/98/NT*. Paper presented at the Nucleic acids symposium series.
- Hemingway, J., & Ranson, H. (2000). Insecticide resistance in insect vectors of human disease. *Annual Review of Entomology*, 45(1), 371–391. <https://doi.org/10.1146/annurev.ento.45.1.371>
- Hunt, R., Brooke, B., Pillay, C., Koekemoer, L., & Coetzee, M. (2005). Laboratory selection for and characteristics of pyrethroid resistance in the malaria vector *Anopheles funestus*. *Medical and Veterinary Entomology*, 19(3), 271–275. <https://doi.org/10.1111/j.1365-2915.2005.00574.x>
- Ibrahim, S. S., Ndula, M., Riveron, J. M., Irving, H., & Wondji, C. S. (2016). The P450 CYP6Z1 confers carbamate/pyrethroid cross-resistance in a major African malaria vector beside a novel carbamate-insensitive N485I acetylcholinesterase-1 mutation. *Molecular Ecology*, 25(14), 3436–3452. <https://doi.org/10.1111/mec.13673>
- Ibrahim, S. S., Riveron, J. M., Bibby, J., Irving, H., Yunta, C., Paine, M. J., & Wondji, C. S. (2015). Allelic variation of cytochrome P450s drives resistance to Bednet insecticides in a major malaria vector. *PLoS Genetics*, 11(10), e1005618. <https://doi.org/10.1371/journal.pgen.1005618>
- Ingham, V. A., Pignatelli, P., Moore, J. D., Wagstaff, S., & Ranson, H. (2017). The transcription factor Maf-S regulates metabolic resistance to insecticides in the malaria vector *Anopheles gambiae*. *BMC Genomics*, 18(1), 669. <https://doi.org/10.1186/s12864-017-4086-7>
- Irving, H., & Wondji, C. S. (2017). Investigating knockdown resistance (kdr) mechanism against pyrethroids/DDT in the malaria vector *Anopheles funestus* across Africa. *BMC Genetics*, 18(1), 76. <https://doi.org/10.1186/s12863-017-0539-x>
- Langmead, B., & Salzberg, S. L. (2012). Fast gapped-read alignment with Bowtie 2. *Nature Methods*, 9(4), 357–359. <https://doi.org/10.1038/nmeth.1923>
- Livak, K. J. (1984). Organization and mapping of a sequence on the *Drosophila melanogaster* X and Y chromosomes that is transcribed during spermatogenesis. *Genetics*, 107(4), 611–634.
- Lucas, E. R., Miles, A., Harding, N. J., Clarkson, C. S., Lawniczak, M. K., Kwiatkowski, D. P., Weetman, D., & Donnelly, M. J., & Anopheles gambiae 1000 Genomes Consortium (2019). Whole-genome sequencing reveals high complexity of copy number variation at insecticide resistance loci in malaria mosquitoes. *Genome Research*, 29(8), 1250–1261. <https://doi.org/10.1101/gr.245795.118>
- Lumjuan, N., Rajatileka, S., Changsom, D., Wicheer, J., Leelapat, P., Prapanthadara, L.-A., Somboon, P., Lycett, G., & Ranson, H. (2011). The role of the *Aedes aegypti* Epsilon glutathione transferases in conferring resistance to DDT and pyrethroid insecticides. *Insect Biochemistry and Molecular Biology*, 41(3), 203–209. <https://doi.org/10.1016/j.ibmb.2010.12.005>
- Martinez-Torres, D., Chandre, F., Williamson, M. S., Darriet, F., Bergé, J. B., Devonshire, A. L., Guillet, P., Pasteur, N., & Pauron, D. (1998). Molecular characterization of pyrethroid knockdown resistance (kdr) in the major malaria vector *Anopheles gambiae* ss. *Insect Molecular Biology*, 7(2), 179–184. <https://doi.org/10.1046/j.1365-2583.1998.72062.x>
- Michel, A. P., Ingrassi, M. J., Schemerhorn, B. J., Kern, M., Le Goff, G., Coetzee, M., Elissa, N., Fontenille, D., Vulule, J., Lehmann, T., Sagnon, N. F., Costantini, C., & Besansky, N. J. (2005). Rangewide population genetic structure of the African malaria vector *Anopheles funestus*. *Molecular Ecology*, 14(14), 4235–4248. <https://doi.org/10.1111/j.1365-294X.2005.02754.x>
- Mitchell, S. N., Stevenson, B. J., Müller, P., Wilding, C. S., Egyir-Yawson, A., Field, S. G., Hemingway, J., Paine, M. J. I., Ranson, H., & Donnelly, M. J. (2012). Identification and validation of a gene causing cross-resistance between insecticide classes in *Anopheles gambiae* from Ghana. *Proceedings of the National Academy of Sciences of the United States of America*, 109(16), 6147–6152. <https://doi.org/10.1073/pnas.1203452109>
- Mugenzi, L. M., Menze, B. D., Tchouakui, M., Wondji, M. J., Irving, H., Tchoupo, M., Hearn, J., Weedall, G. D., Riveron, J. M., & Wondji, C. S. (2019). Cis-regulatory CYP6P9b P450 variants associated with loss of insecticide-treated bed net efficacy against *Anopheles funestus*. *Nature Communications*, 10(1), 1–11.
- Nardini, L., Holm, I., Pain, A., Bischoff, E., Gohl, D. M., Zongo, S., Guelbeogo, W. M., Sagnon, N., Vernick, K. D., & Riehle, M. M. (2019). Influence of genetic polymorphism on transcriptional enhancer activity in the malaria vector *Anopheles coluzzii*. *Scientific Reports*, 9(1), 1–14. <https://doi.org/10.1038/s41598-019-51730-8>
- Pennacchio, L. A., Bickmore, W., Dean, A., Nobrega, M. A., & Bejerano, G. (2013). Enhancers: Five essential questions. *Nature Reviews Genetics*, 14(4), 288–295. <https://doi.org/10.1038/nrg3458>
- Riveron, J. M., Chiumia, M., Menze, B. D., Barnes, K. G., Irving, H., Ibrahim, S. S., Weedall, G. D., Mzilahowa, T., & Wondji, C. S. (2015). Rise of multiple insecticide resistance in *Anopheles funestus* in Malawi: A

- major concern for malaria vector control. *Malaria Journal*, 14(1), 344. <https://doi.org/10.1186/s12936-015-0877-y>
- Riveron, J. M., Huijben, S., Tchagga, W., Tchouakui, M., Wondji, M. J., Tchoupo, M., Irving, H., Cuamba, N., Maquina, M., Paaïmans, K., & Wondji, C. S. (2019). Escalation of pyrethroid resistance in the malaria vector *Anopheles funestus* induces a loss of efficacy of PBO-based insecticide-treated nets in Mozambique. *Journal of Infectious Diseases*, 220, 467–475. <https://doi.org/10.1093/infdis/jiz139>
- Riveron, J. M., Ibrahim, S. S., Mulamba, C., Djouaka, R., Irving, H., Wondji, M. J., Ishak, I. H., & Wondji, C. S. (2017). Genome-wide transcription and functional analyses reveal heterogeneous molecular mechanisms driving pyrethroids resistance in the major malaria vector *Anopheles funestus* across Africa. *G3: Genes, Genomes, Genetics*, 7, 1819–1832.
- Riveron, J. M., Irving, H., Ndula, M., Barnes, K. G., Ibrahim, S. S., Paine, M. J., & Wondji, C. S. (2013). Directionally selected cytochrome P450 alleles are driving the spread of pyrethroid resistance in the major malaria vector *Anopheles funestus*. *Proceedings of the National Academy of Sciences of the United States of America*, 110(1), 252–257. <https://doi.org/10.1073/pnas.1216705110>
- Riveron, J. M., Yunta, C., Ibrahim, S. S., Djouaka, R., Irving, H., Menze, B. D., Ismail, H. M., Hemingway, J., Ranson, H., Albert, A., & Wondji, C. S. (2014). A single mutation in the GSTe2 gene allows tracking of metabolically-based insecticide resistance in a major malaria vector. *Genome Biology*, 15(2), R27. <https://doi.org/10.1186/gb-2014-15-2-r27>
- Weedall, G. D., Mugenzi, L. M. J., Menze, B. D., Tchouakui, M., Ibrahim, S. S., Amvongo-Adjia, N., Irving, H., Wondji, M. J., Tchoupo, M., Djouaka, R., Riveron, J. M., & Wondji, C. S. (2019). A cytochrome P450 allele confers pyrethroid resistance on a major African malaria vector, reducing insecticide-treated bednet efficacy. *Science Translational Medicine*, 11(484), eaat7386.
- Weedall, G. D., Riveron, J. M., Hearn, J., Irving, H., Kamdem, C., Fouet, C., White, B. J., & Wondji, C. S. (2020). An Africa-wide genomic evolution of insecticide resistance in the malaria vector *Anopheles funestus* involves selective sweeps, copy number variations, gene conversion and transposons. *PLoS Genetics*, 16(6), e1008822.
- Wei, Z., Wang, W., Hu, P., Lyon, G. J., & Hakonarson, H. (2011). SNVer: A statistical tool for variant calling in analysis of pooled or individual next-generation sequencing data. *Nucleic Acids Research*, 39(19), e132. <https://doi.org/10.1093/nar/gkr599>
- WHO (2012). *Global plan for insecticide resistance management in malaria vectors: executive summary*, Geneva, Switzerland: World Health Organization. Retrieved from <https://apps.who.int/iris/handle/10665/44846>
- WHO (2013). *Malaria entomology and vector control*, Geneva, Switzerland: World Health Organization. <https://www.who.int/malaria/publications/atoz/9789241505819/en/>
- WHO (2018). *World malaria report 2018*, Geneva, Switzerland: World Health Organization. <https://www.who.int/malaria/publications/world-malaria-report-2018/en/>
- WHO (2019). *World malaria report 2019*, Geneva, Switzerland: World Health Organization. <https://www.who.int/publications-detail-redirect/9789241565721>
- Wilding, C. S., Smith, I., Lynd, A., Yawson, A. E., Weetman, D., Paine, M. J., & Donnelly, M. J. (2012). A cis-regulatory sequence driving metabolic insecticide resistance in mosquitoes: Functional characterisation and signatures of selection. *Insect Biochemistry and Molecular Biology*, 42(9), 699–707. <https://doi.org/10.1016/j.ibmb.2012.06.003>
- Wondji, C. S., Dabire, R. K., Tukur, Z., Irving, H., Djouaka, R., & Morgan, J. C. (2011). Identification and distribution of a GABA receptor mutation conferring dieldrin resistance in the malaria vector *Anopheles funestus* in Africa. *Insect Biochemistry and Molecular Biology*, 41(7), 484–491.
- Wondji, C. S., Irving, H., Morgan, J., Lobo, N. F., Collins, F. H., Hunt, R. H., Coetzee, M., Hemingway, J., & Ranson, H. (2009). Two duplicated P450 genes are associated with pyrethroid resistance in *Anopheles funestus*, a major malaria vector. *Genome Research*, 19, 452–459.

SUPPORTING INFORMATION

Additional supporting information may be found online in the Supporting Information section.

How to cite this article: Mugenzi LMJ, Menze BD, Tchouakui M, et al. A 6.5-kb intergenic structural variation enhances P450-mediated resistance to pyrethroids in malaria vectors lowering bed net efficacy. *Mol Ecol* 2020;29:4395–4411. <https://doi.org/10.1111/mec.15645>